J Mater Sci (2006) 41:6280–6289
DOI 10.1007/s10853-006-0506-9

Quasi-static and dynamic compressive behaviour of poly(methyl methacrylate) and polystyrene at temperatures from 293 K to 363 K

S. F. Lee · G. M. Swallowe

Received: 19 March 2004 / Accepted: 1 September 2005 / Published online: 12 August 2006

Abstract Flow stress, Young's Modulus, energy and strain of fracture of poly(methyl methacrylate) (PMMA) and polystyrene (PS) were studied under compressive loading at strain rates of 10^{-4}–10 s^{-1} and temperatures from 293 K to temperatures ~20 K below T_g. It was found that the energy of fracture shows an increase in the quasi-static strain rate (10^{-4}–10^{-3} s^{-1}) region and becomes constant in the low strain rate (10^{-2}–10 s^{-1}) region, while the strain of fracture shows a slow decrease with rate over the strain rate range tested. The activation energies and volumes of PMMA and PS at yield stress, 20% and 30% strain were evaluated using Eyring's theory of viscous flow. ΔG was found to be constant for all strain rates and strains for both PMMA and PS. The activation volume for both materials increased as a function of strain.

Introduction

In this work, the mechanical behaviour under compression of two commercially important fully atactic amorphous polymers, poly(methyl methacrylate) (PMMA) and polystyrene (PS) has been studied. Although both materials have been extensively studied in the past [1, 2] most of the previous work has been carried out under tension. The aim of the work described in this paper is to gather a comprehensive set of compressive data for these two materials over a wide strain rate range and to study the effect of strain rate and temperature on the stress–strain properties and the strain to failure.

Yield stress has been defined in several ways [3–5]. PMMA and PS initially display a linear increase of stress with increasing strain, followed by a maximum stress after the elastic limit, undergo a fall in stress, in tension experience cold drawing, strain hardening and then fracture. The maximum stress after the elastic limit in the stress–strain curves of PMMA and PS is taken as yield stress in this study.

When a material is subjected to compressive or tensile tests, some of the work of deformation will appear as heat. Temperature rises occur in the material if the heat developed is not lost to the surroundings. In polymeric materials, which are very sensitive to strain rate and temperature, the heat developed during deformation can affect the stress–strain curve if it is not quickly dissipated. The temperature rise will produce softening and cause a change in the mechanical properties [6]. Adiabatic heating will only produce a marginal effect on the modulus and the yield stress but will be of increasing importance as deformation continues and increasing amounts of plastic work take place in the material. Provided expression 1 [7] holds a test can be considered to be isothermal.

$$\dot{\gamma} < \frac{2\kappa}{L^2} \tag{1}$$

with γ the shear strain, κ the thermal diffusivity and L the length scale of the sample. Calculations for the samples used in this work show that experiments will begin to deviate from isothermal conditions when the strain rate exceeds 0.05. An estimate of the temperature rise occurring during plastic deformation can be

S. F. Lee · G. M. Swallowe (✉)
Department of Physics, Loughborough University,
Leicestershire LE11 3TU, UK
e-mail: G.M.Swallowe@lboro.ac.uk

obtained by integrating under the stress–strain curve and equating the plastic work to thermal energy.

$$\Delta T = \frac{\int \sigma d\varepsilon}{\rho C_p} \quad (2)$$

The density of PMMA (ρ) is taken to be 1,190 kg m^{-3} and PS to be 1,050 kg m^{-3}. The heat of capacity of PMMA (C_p) is found from the DSC measurements to be 840 J kg^{-1} K^{-1} at 323 K and 970 J kg^{-1} K^{-1} at 343 K, respectively. The heat capacity of PS was measured as 530 kg m^{-3} at 323 K and 680 kg m^{-3} at 353 K.

Based on the stress–strain data obtained this would lead to predicted temperature rises of ~13 °C for PMMA at 343 K at a strain rate of 0.5 s^{-1} and a strain of 0.3 rising to ~35 °C at 293 K for the same strain and strain rate. For PS the predicted temperature increase are ~10 °C at 353 K and ~21 °C at 293 K for the same strain and strain rate. Lower rates will lead to considerably lower temperature rises since the time scale will be such that heat diffusion will dominate and additionally the flow stress, and hence energy dissipation will be smaller. These temperature rise calculations assume adiabatic conditions and full conversion of work to heat. This is found to apply accurately during high rate deformation in metals. However, even at high rates all the 'plastic' work is rarely converted into heat in polymers and the remainder is stored as elastic strain energy in the material. Typical average conversion factors for polycarbonate in high rate tests are 35% at a strain of 0.1 increasing to 80% at a strain of 0.4 and then falling off to only 20% at high strains [8]. Since polycarbonate is another fully amorphous polymer it is assumed that the behaviour of polycarbonate will be representative of the polymers used in this work. The temperature rises quoted above must therefore be regarded as maximum possible estimates and the actual values are expected to amount to less than half of those quoted. In this work temperature rises are only expected to pose a problem for strains in excess of 0.1 and strain rates greater than 0.1 s^{-1}.

Experimental procedure

Samples

The materials used in the tests were all from single batches of PMMA and PS purchased from Goodfellow Cambridge Limited. The samples were prepared from as received commercial stock. PMMA samples were made from 6 mm diameter cylindrical rod by using a parting tool. They formed accurate right cylinders of height 3.0 mm. PS samples were machined into 8.0 mm diameter right cylinder from sheet of 4.0 mm thickness. Surface flatness was better 0.05 mm in all cases. Aspect ratio 2:1 was maintained for all samples. No polishing or annealing of the prepared samples was carried out. Both materials were studied using a Mettler DSC and the glass transition temperatures of PMMA and PS were found to be 390 K and 373 K, respectively.

Mechanical tests

Uniaxial compression was performed on the samples using a conventional Hounsfield H50KM Universal Test Machine, (quasi-static (isothermal) tests were carried out over the strain rate range, 10^{-4}–10^{-1} s^{-1}, and low strain rate (non-isothermal) tests over the range 10^{-1}–10 s^{-1}). In all tests a layer of petroleum jelly was applied to both sample surfaces to achieve uniform compression and avoid barrelling [9]. Strain rates were evaluated by plotting strain against time for the whole test and taking the strain rate as the tangent in the section immediately after yield. In practice these plots were only slightly curved and the strain rate varied by no more than a factor of 2 throughout the test.

In order to reach thermal equilibrium in elevated temperature tests, samples were heated for 30 min before the test, with the aid of a thermostatically controlled heating block surrounding the steel platens between which the sample was compressed. The chosen testing temperature ranges were from 293 K to 363 K for PMMA and from 293 K to 353 K for PS. The highest testing temperature was chosen at around 20 K below the glass transition temperature since the samples relaxed from their initial shape prior to compression when heated at temperatures closer to the glass transition temperature.

Strain limited tests [10] were used to halt the compression during selected tests so that the birefringence of samples tested to different strains could be measured. These limits were achieved with the aid of steel rings which encircled the samples and halted the test when the upper platen came into contact with the ring. Four strain limits, which are 0.2, 0.4, 0.6 and 0.8, were chosen. Since the thickness of PMMA and PS were 3 and 4 mm respectively, metal rings with eight different thicknesses were constructed. The thickness of the rings used to stop further strain in the PMMA samples were 2.45, 2.00, 1.64 and 1.34 mm; for PS they were 3.00, 2.50, 2.03 and 1.65 mm thick.

In this study, the true stress and true strain were calculated using $\sigma_t = \frac{F_t}{A_t}$ and $\varepsilon_t = \int_{h_0}^{h_t} \frac{dh}{h} = \ell n\left[\frac{h_t}{h_0}\right]$ where the subscript t refers to the instantaneous force F_t,

sample area A_t and height h_t at time t. The volume of the tested sample was assumed to be constant during plastic deformation. Figure 1 shows the stress–strain curves of PMMA and PS until fracture at different strain rates.

In this work, involving both quasi-static and dynamic compression, Young's modulus is taken as the gradient of the stress–strain curve at a strain of 0.02. Up to this strain the applied stress is, to a good approximation, linearly proportional to strain in all the stress–strain curves. The energy of fracture is calculated by integrating the area under stress–strain curve until fracture and the strain of fracture is taken as strain where polymer fracture commences. In most cases the applied force showed a sudden drop when the sample fractured and the fracture stress was easy to identify. However, at the highest strain rates when the compressing platen was moving rapidly, it continued to compress the samples after they had fractured causing difficulties in accurately determining the strain at which the samples fractured. Fracture strain data from these higher rate tests are not included in the results presented.

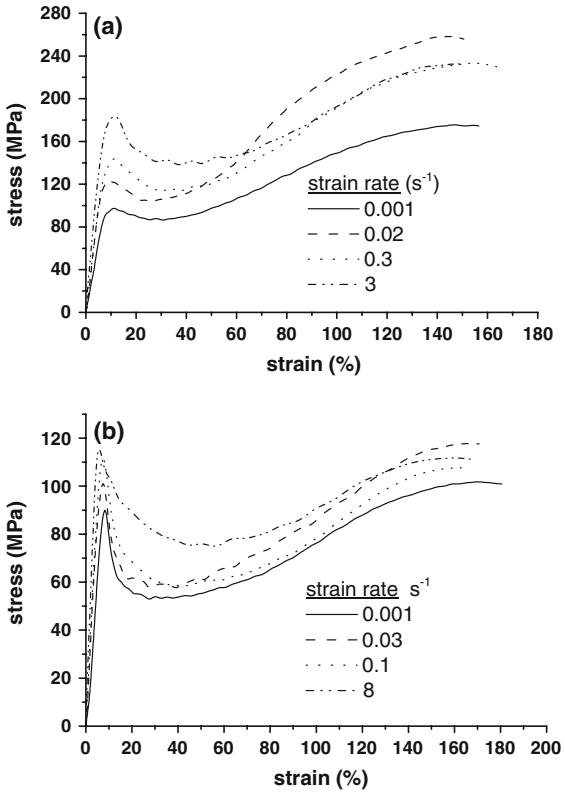

Fig. 1 Stress–strain curves of (**a**) poly(methyl methacrylate) and (**b**) polystyrene until fracture at 293 K and different strain rates. Results are averages of at least three samples. Accuracy typically ±3 MPa

Birefringence measurement and microscopy

A Carl Zeiss 431 polarising microscope was used to view and measure the birefringence of samples tested to different strain limits. The compressed and uncompressed samples of PMMA and PS were swept with a layer of Cargille liquid, which has a refractive index roughly same as that of the sample, to reduce refraction caused by microcracks found on both surfaces of the sample. The samples were placed on the microscope stage with their cylinder-axes parallel to the microscopic axis. A Carl Zeiss 4894000 Erhinghaus rotary compensator was used to measure the optical path differences of the emergent light and monitor its change in the compressed samples. The birefringence is defined as a measure of the difference in refractive indices in two mutually perpendicular directions and was calculated as

$$\Delta n = \left| n_{\text{high}} - n_{\text{low}} \right| = \frac{\text{OPD}}{t} \tag{3}$$

where t is the thickness of the sample and OPD is the optical path difference of light emerging from the top surface of the sample. The magnitude but not the sign of the birefringence was recorded. The purpose of these tests was to search for trends in birefringence as a function of strain rate and temperature of testing. It is recognised that some recovery of the samples will occur between the end of the tests and the birefringence measurements. However, when tested well below T_g recovery is very slow and the strain recovery in the samples was measured to be around 2%–4% for samples tested to strains of 0.2 and 0.4 and 5%–10% for samples tested to strains of 0.6 and 0.8. Since this recovery is only a small fraction of the sample strains at the end of the tests it is believed that the birefringence measurements will be representative of the state of the samples at the end of the test. The results of the measurements are listed in Table 1.

The topological surfaces of the compressed samples at four different strains (0.2, 0.4, 0.6 and 0.8) at different rates were studied using a LEO 1530VP Scanning Electron Microscope (SEM) after coating them with a thin layer of aluminium on both surfaces.

DMTA analysis

Dynamic mechanical thermal analysis was performed on rectangular bars of PMMA and PS with dimensions of $17.5 \times 10.5 \times 1.9$ mm^3 to study the effect of strain rate on the β transition. The machine used was a Polymer Laboratories Dynamic Mechanical Thermal

Table 1 Birefringence of PMMA tested at different strain rates and at different temperatures using the Hounsfield Machine

T (K)	$\dot{\varepsilon}$ (s^{-1})	Birefringence at different strain × 10^4			
		0.8	0.6	0.4	0.2
293	0.0006	2.6	3.0	1.6	–
	0.006	2.4	1.3	0.0	–
	0.05	2.9	1.4	0.1	–
	0.5	4.5	3.3	2.2	–
323	0.0006	2.4	3.5	2.3	2.4
	0.006	2.0	2.6	2.5	2.1
	0.05	5.6	4.7	2.2	1.4
	0.5	5.8	4.4	2.5	0.1
343	0.0006	1.0	1.6	1.3	1.1
	0.006	2.0	1.8	1.6	2.3
	0.05	2.8	3.2	2.9	1.3
	0.5	4.6	3.9	3.5	0.7

Measurement accuracy ~±10%

Analyser (PL-DMTA). All measurements were carried out at two frequencies, namely 0.1 Hz and 100 Hz. The heating rate was set at 3 °C/min and specimens were tested over the temperature range from −100 °C to the temperature at which the specimens were found to have become excessively softened and could not be properly flexed.

For PMMA tested at 0.1 Hz, the broad peak of β relaxation is between −50 °C and 25 °C (Fig. 2—dash line), while at 100 Hz is around 35 °C–70 °C (Fig. 2—solid line). The β relaxation in PMMA is generally due to the movement of the ester group in the polymer. For polystyrene tested at 0.1 Hz, a very broad peak was observed at the temperature between −25 °C and 25 °C. It could be due to the β relaxation of polymer chains in PS (Fig. 3—dash line). However, at 100 Hz, the peak disappeared (Fig. 3—solid line). Illers [11] reported the β relaxation peak merges with the α relaxation at frequencies higher than 40 Hz. Illers

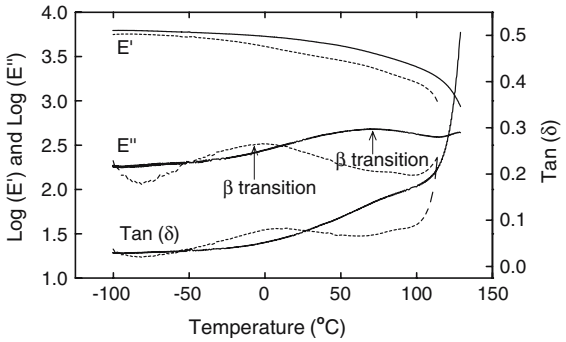

Fig. 2 Storage modulus (E' GPa), loss modulus (E'' GPa) and loss tangent (tan(δ)) of PMMA at 0.1 Hz (*dash line*) and 100 Hz (*solid line*)

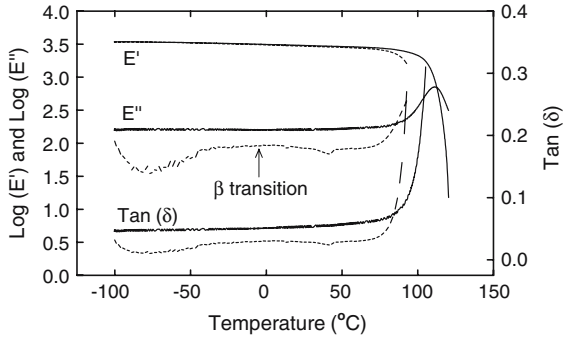

Fig. 3 Storage modulus (E' GPa), loss modulus (E'' GPa) and loss tangent (tan(δ)) of PS at 0.1 Hz (*dash line*) and 100 Hz (*solid line*)

and Jenckel [12] said that the β relaxation is due to the rotation of same phenyl groups, which possess less steric hindrance than others. The strains imparted to the samples in the DMTA are very small ~10^{-2}, therefore the strain rates at 0.1 Hz and 100 Hz correspond to ~10^{-3} s^{-1} and 1 s^{-1}.

Application of Eyring's theory

Models based on Eyring's equation for viscous flow have been successful in explaining the strain rate and temperature response of plastic flow in polymers. In these models polymer chains surmount a potential barrier, characterised by an activation energy, to release the stress in order to achieve equilibrium. The volume involved in the chain movement is called the activation volume. The process is thermally activated and the simplest expression to describe the process is given as

$$\frac{\sigma}{T} = \frac{4k}{\upsilon_a}\left(\ln\dot{\varepsilon} - \ln\frac{2}{3}\frac{\upsilon_a}{\upsilon_m}\frac{kT}{h} + \frac{\Delta G}{RT}\right) \tag{4}$$

where σ is the applied stress, T the temperature, k Boltzmann's constant, h Planck's constant, R the gas constant, $\dot{\varepsilon}$ the strain rate, υ_a the activation volume, υ_m the molecular chain volume and ΔG the activation energy [13]. It is assumed that spaces must exist in the system for flows to occur [14]. Many authors [15–18] have applied the Eyring equation at the yield stress. In this study, plots of σ/T against $\ln\dot{\varepsilon}$ were carried out not only on the yield point, but also at 20% and 30% strain. These strains are within the lower yield range. Nanzai [19], studying the transient stress–strain relation of poly(methyl methacrylate) at 100 °C by decreasing and increasing the strain rate by a factor of 0.01, revealed that a state of steady flow was shown in the lower yield range which can be analysed quantitatively using the Eyring equation.

As predicted by Eq. (4) plots of σ/T against $\ln\dot{\varepsilon}$ produced straight lines in all cases for PS. The method adopted by Bauwens-Crowet et al. [20] was used to calculate the activation energy and volume at the yield point, 20% and 30% strain. The results are presented in Table 2.

As has been observed by other workers [18, 19] the plots of σ/T against $\ln\dot{\varepsilon}$ for PMMA produced curves and application of the Bawens-Crowet method to calculate ΔG and υ_a is therefore impossible. In this study, rather than assume multiple activation energies and volumes the partial derivatives method proposed by Zhu et al. [18] was adopted to evaluate ΔG and υ_a. In this method ΔG in Eq. (4) is substituted by $(\Delta H - T\Delta S)$ with ΔH the activation enthalpy and ΔS the activation entropy. υ_a is calculated by taking partial derivatives of σ/T with respect to $\ln(\dot{\varepsilon})$ under constant T, assuming that, to a first approximation ΔH and ΔS do not vary with greatly with $\dot{\varepsilon}$ and T.

$$\left(\frac{\partial(\sigma/T)}{\partial\ln(\dot{\varepsilon})}\right)_T = \frac{4k}{\upsilon_a} \tag{5}$$

Taking the partial derivatives of σ/T with respect to $1/T$ under constant $\underline{\varepsilon}$ enables ΔH to be evaluated knowing υ_a using Eq. (6)

$$\left(\frac{\partial(\sigma/T)}{\partial(1/T)}\right)_{\dot{\varepsilon}} = \frac{4k}{\upsilon_a}\left(\frac{\Delta H}{R} + T\right) \tag{6}$$

The gradients are evaluated from fitted curves to the experimental data. ΔS can be calculated from Eq. (4) when the values of ΔH and υ_a are known. Table 3 lists values of $\Delta G = (\Delta H - T\Delta S)$ and υ_a as a function of strain rate, strain and temperature for PMMA.

Table 2 The activation volume and energy for polystyrene at yield, 20% and 30% strain

	Activation volume, υ_a (nm^3) ± 5%			Activation energy, ΔG (kJ mol^{-1}) ± 15%
	293 K	323 K	353 K	
Yield	3.6	4.0	4.3	193
20% strain	5.2	7.6	8.8	277
30% strain	8.6	10.1	10.4	310

Table 3 The activation volume and energy of poly(methyl methacrylate) at (a) yield strain, (b) 20% strain and (c) 30% strain at five different temperatures

$\ln(\dot{\varepsilon}_y)$	Activation volume, υ_a (nm^3)					Activation energy, ΔG (kJmol^{-1})				
	293 K	311 K	323 K	343 K	363 K	293 K	311 K	323 K	343 K	363 K
(a)										
−6.5	1.9	2.8	5.0	12.2	17.9	104	89	104	126	109
−5.5	1.6	2.2	3.5	5.6	7.2	99	85	94	93	89
−4.5	1.5	1.9	2.8	3.6	4.5	96	83	89	85	85
−3.5	1.3	1.6	2.3	2.7	3.3	93	82	87	83	84
−2.5	1.2	1.4	1.9	2.1	2.6	90	82	85	82	84
−1.5	1.1	1.3	1.7	1.8	2.1	88	82	85	82	85
−0.5	1.0	1.1	1.5	1.5	1.8	85	82	84	83	85
0.3	1.0	1.0	1.3	1.4	1.6	84	82	84	84	85
(b)										
−6.5	2.1	4.6	4.8	25.2	31.2	104	103	90	161	91
−5.5	2.0	3.5	3.9	8.5	11.0	103	94	88	97	85
−4.5	1.9	2.9	3.2	5.1	6.7	101	89	86	86	84
−3.5	1.9	2.4	2.8	3.7	4.8	100	87	86	82	83
−2.5	1.8	2.1	2.4	2.9	3.8	98	85	85	81	84
−1.5	1.7	1.8	2.2	2.3	3.1	97	84	85	80	84
−0.5	1.6	1.6	1.9	2.0	2.6	95	83	86	80	85
0.3	1.3	1.5	1.8	1.8	2.3	94	83	86	81	86
(c)										
−6.5	2.9	4.8	7.1	–	–	116	102	109	–	–
−5.5	2.7	3.8	5.2	13.2	22.2	112	95	99	119	111
−4.5	2.5	3.2	4.1	6.4	8.6	108	91	94	92	87
−3.5	2.3	2.7	3.4	4.3	5.3	105	89	91	85	84
−2.5	2.1	2.4	2.9	3.2	3.8	102	87	89	82	83
−1.5	2.0	2.1	2.5	2.5	3.0	99	86	88	81	83
−0.5	1.8	1.9	2.2	2.1	2.5	97	86	87	81	84
0.3	1.7	1.7	2.0	1.9	2.2	95	86	87	81	84

Accuracy of υ_a typically ±7%, of ΔG ±15%

Results

Figures 4 and 5 illustrate the relationship between yield stress and strain rate for PMMA and PS at quasi-static and low strain rates. At all temperatures the yield stress of PMMA shows a non-linear increase with log of strain rate while that of PS shows a linear increase. The PMMA data could be very well fitted using an expression of the form

$$\sigma/T = A\exp(B\ln\dot{\varepsilon}) + C \tag{7}$$

with A, B, C constants. This is written in a mathematically clumsy form but conveniently shows that for PMMA σ/T does not vary linearly with $\ln\dot{\varepsilon}$. All three constants were different for data obtained at different temperatures. The flow stresses of PMMA and PS at 20% (Figs. 4b, 5b) and 30% strain (Figs. 4c, 5c) followed the same trend as that of the yield stress versus log strain rate data.

Figures 6, 7, 8 and 9 show the Young's modulus, energy and strain of fracture of PMMA and PS against $\ln\dot{\varepsilon}$. Although the results are rather scattered it is evident that there is a steady increase in modulus as a function of strain rate and that the relationship between modulus and $\ln\dot{\varepsilon}$ follows the same form as Eq. (7). A similar pattern can be seen in the PS data although it is even more scattered and no reliable fits can be made. There is no clear dependence of strain of fracture on strain rates for PMMA and PS. The results for PMMA are scattered but appear to show a slow decrease until the strain

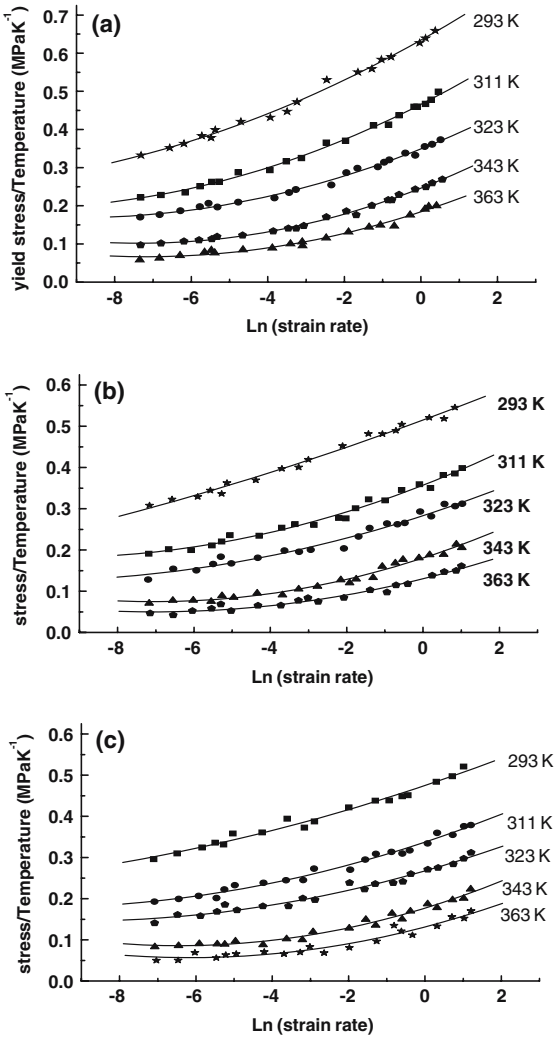

Fig. 4 Stress/Temperature versus ln(strain rate) at (**a**) yield point, (**b**) 20% strain and (**c**) 30% strain for poly(methyl methacrylate) tested at low strain rates 10^{-4}–2 s^{-1} at various temperatures. Accuracy of σ/T typically ±0.01

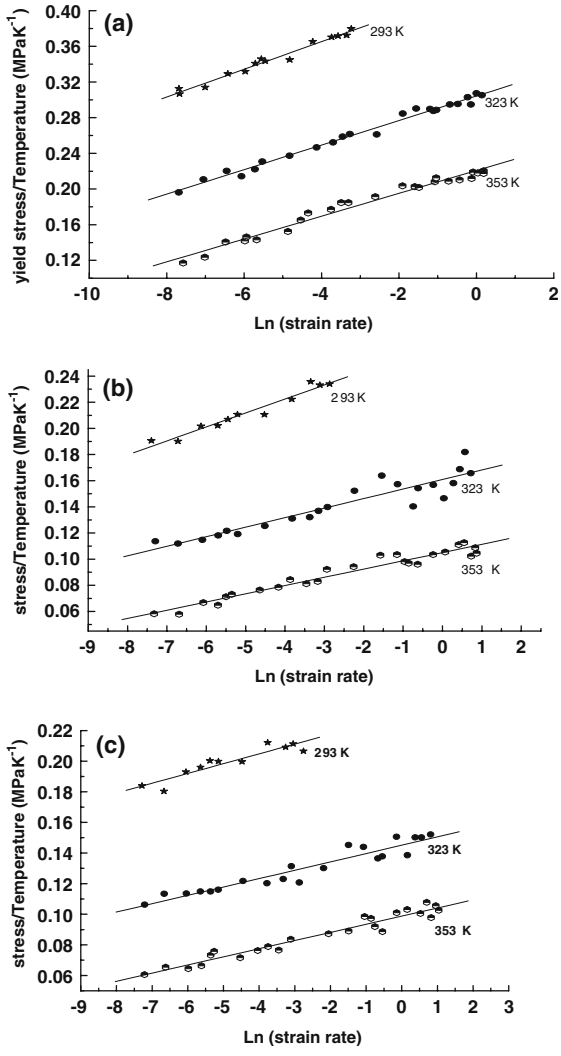

Fig. 5 Stress/Temperature versus ln(strain rate) at (**a**) yield point, (**b**) 20% strain and (**c**) 30% strain for polystyrene tested at low strain rates 10^{-4}–2 s^{-1} at various temperatures. Accuracy of σ/T typically ±0.01

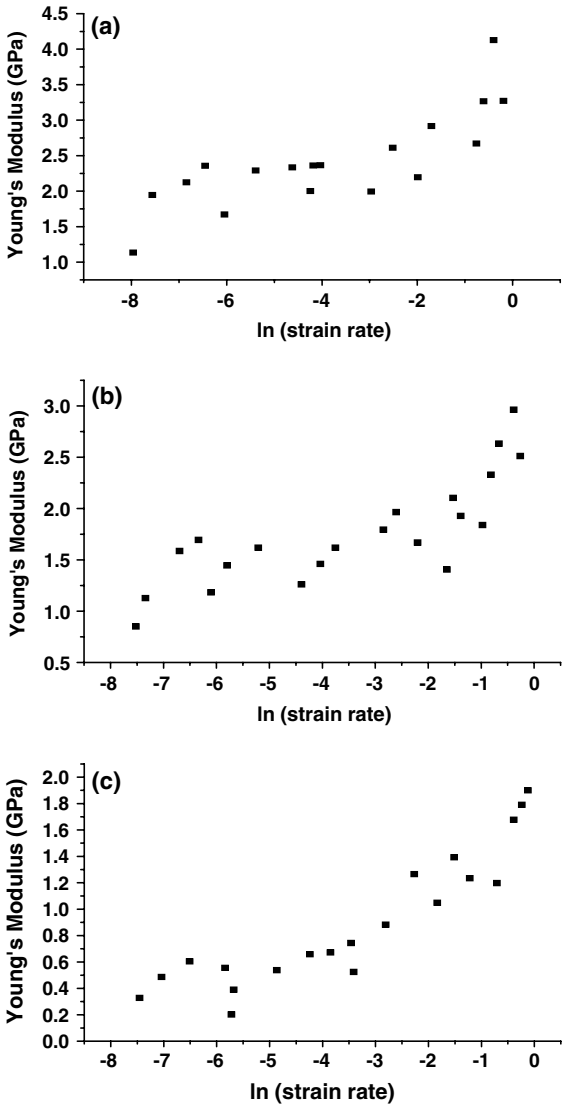

Fig. 6 Young's Modulus versus ln(strain rate) for poly(methyl methacrylate) at temperatures of (**a**) 293 K, (**b**) 323 K and (**c**) 363 K. Accuracy typically ±0.1 GPa

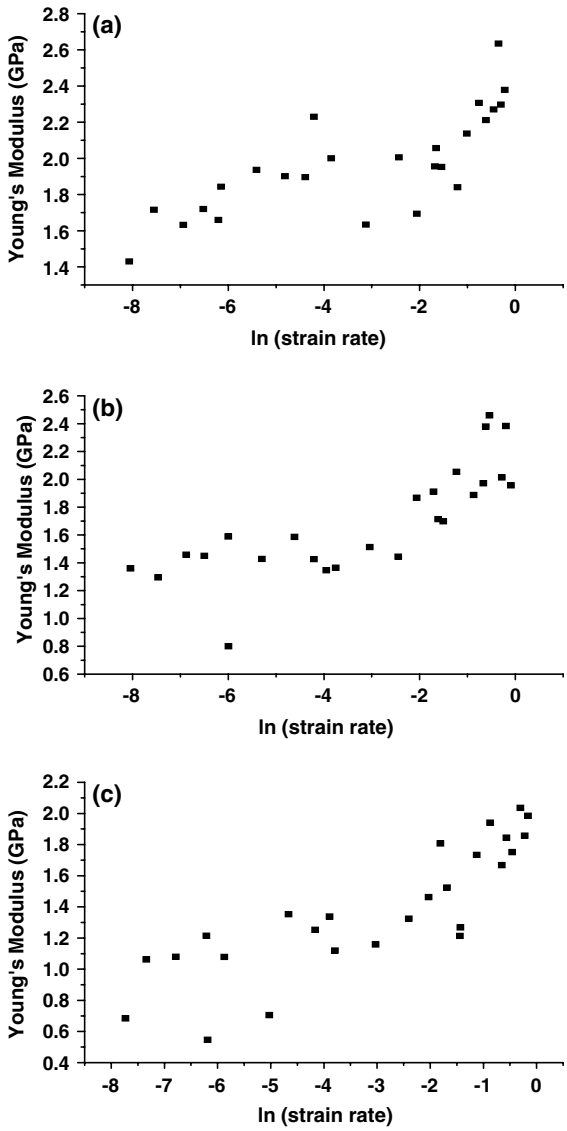

Fig. 7 Young's Modulus versus ln(strain rate) for polystyrene at temperatures of (**a**) 293 K, (**b**) 323 K and (**c**) 353 K. Accuracy typically ±0.1 GPa

rates reach ~0.4 after which the fracture strain falls more rapidly. The energy absorbed by PMMA before fracture shows an increase with strain rate and decrease with temperature. This arises from the increase in flow stress combined with the rather slow decrease in fracture strain with strain rate leading to increasing values of $\sigma d\varepsilon$. Increasing temperature decreases the flow stress at a rate which is not compensated for by a sufficiently large increase in fracture strain and hence the energy decreases. Since much of this energy is stored as elastic strain energy in the polymer these plots can be taken as representative of the energy available to cause fracture. The PS data is again very scattered but the same trends as are observed in PMMA are seen.

Examples of the birefringence patterns, which are related to the chain orientation of uncompressed and compressed samples of PMMA, are shown in Fig. 10. The samples were made from 'as-received' material and were not initially isotropic. Dark crosses were seen on compressed samples and became wider with increasing strain. Birefringence data are presented in Table 1. The light 'ring' observed around the samples in Fig.10 is due to a crazed and cracked region forming around the circumference which grows as a function of strain. The faint outer rings are due to the Cargille liquid used to reduce refraction from microcracks. Only the PMMA samples provided reliable birefringence measurements. The PS samples had a multicoloured speckled appearance indicating

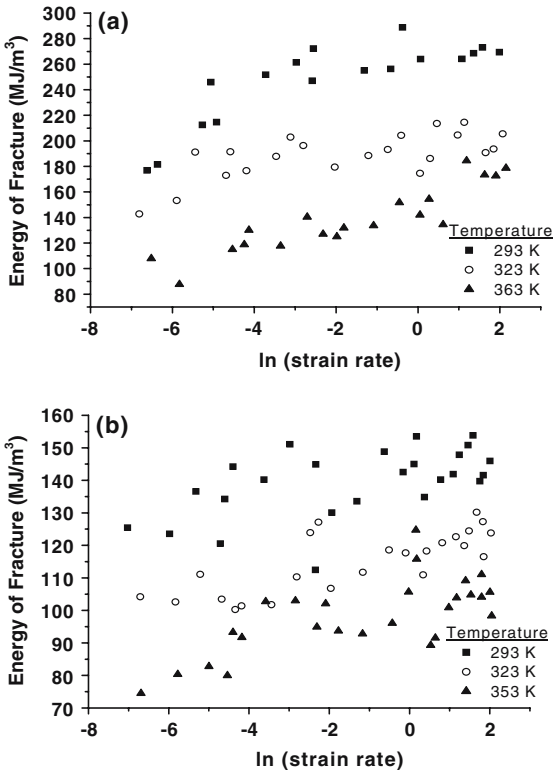

Fig. 8 Energy of fracture versus ln(strain rate) for (**a**) poly(methyl methacrylate) and (**b**) polystyrene at three different temperatures. Accuracy typically ±10 MJ m^{-3}

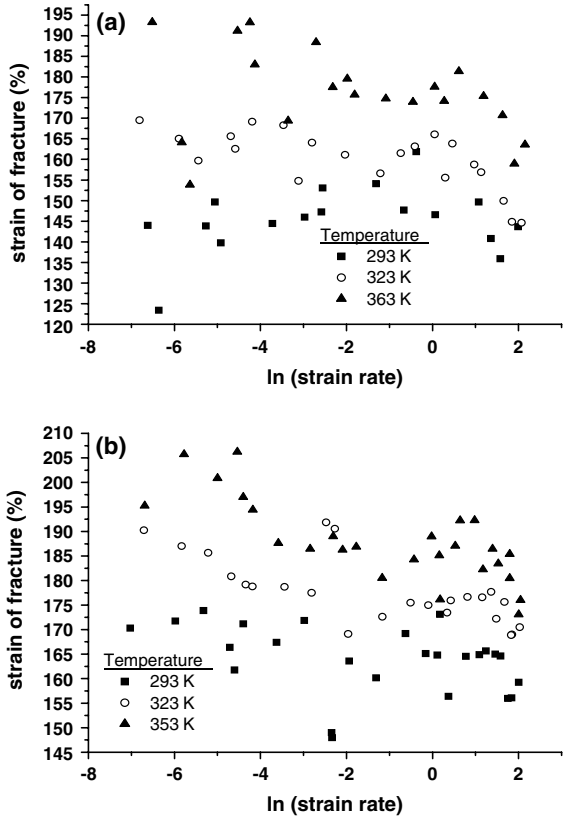

Fig. 9 Strain of fracture versus ln(strain rate) for (**a**) poly (methyl methacrylate) and (**b**) polystyrene at three different temperatures

anisotropy on a much smaller scale. Electron microscope studies of the surface of the PMMA samples compressed to four different strains at different rates (0.2, 0.4, 0.6 and 0.8) showed that cracked or crazed regions developed from the edges of the samples (Fig. 11) to form a ring around the rest of the material when the strain exceeded 0.2. Figure 11 shows a section of this cracked/crazed ring. The region to the left of the cracked region in Fig. 11 is plastically deformed but uncrazed polymer. With increased strain the ring continues to grow inwards until failure of the whole sample occurs either by multiple shear or by cracking of the central region.

Discussion

It is evident from the results presented in Table 1 that the birefringence of PMMA does not show any consistent dependence on strain, strain rate or temperature. This is a little surprising since the uniform expansion of the sample during compression should give rise to radial orientation in the plane of the sample. The greatest value of birefringence seems to be found at 323 K, at higher strain and at higher strain rates. The birefringence was rather small and it may be that the sensitivity of the measurements were not sufficient to follow any changes. It is clear from the photographs that a ring with birefringence different from the central section of the sample grows inwards as a function of strain. Close examination shows many radial cracks in this region. Strain relief caused by this cracking is the cause of the abrupt change in the birefringence observed in the ring around the samples (Figs. 10, 11).

Analysis of the results for PS showed that ΔG was approximately constant independent of temperature and strain rate but that it did increase with strain and that the activation volume υ_a increased with both temperature and strain rate. Results are shown in Table 2. The partial differential calculation method produces a series of activation enthalpy, entropy and volumes for the PMMA flow units as a function of temperature strain and strain rate. The analysis showed variations in ΔH and ΔS with T and $\dot{\varepsilon}$. However, $\Delta G = \Delta H - T\Delta S$ shows a comparatively constant value independent of strain, strain rate and temperature. The activation energy and volume involved in the deformation of PMMA at three different strains are shown in Table 3.

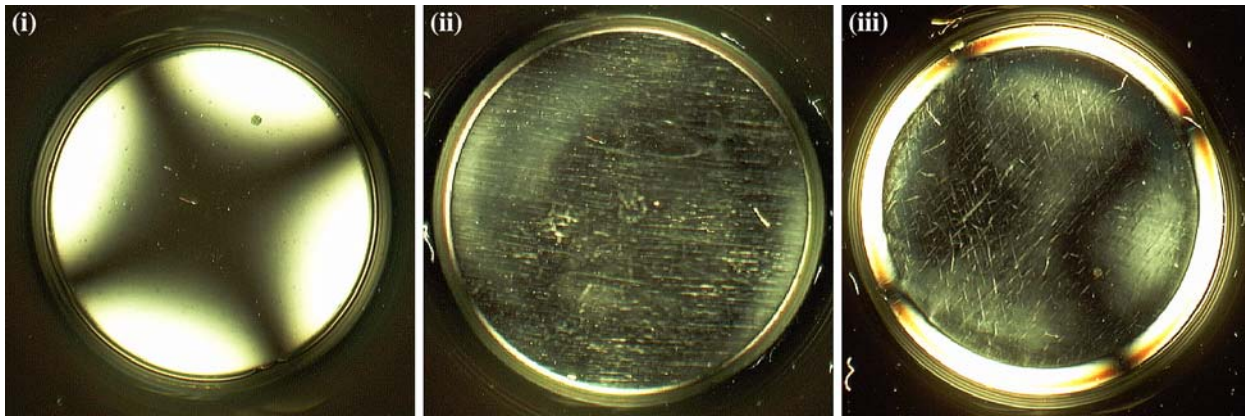

Fig. 10 Interference pattern of PMMA sample and compressed PMMA samples at 293 K and strain rate 0.5 s^{-1} (i) Uncompressed, (ii) strain 0.2, (iii) strain 0.8

Ward's modification of the Eyring theory incorporating an additional pressure activation volume [3], and the Argon theory of polymer yield [21], lead to the conclusion that ΔG should increase linearly with hydrostatic pressure. Since the component of hydrostatic pressure in a compression test can, to a first approximation, be taken to be proportional to the flow stress and the flow stress beyond yield at a given temperature is observed to increase with strain rate one would expect an increase of ΔG (20%) and ΔG (30%) with strain rate. This is not observed in this work.

A comparison of the DMTA data for both materials with the Young's modulus measured from the stress–strain curves shows that the relationship

$$E(\varepsilon, T) = E_0(T)\left(1 - \frac{\varepsilon}{\varepsilon_y}\right) \tag{8}$$

with $E(\varepsilon,T)$ the modulus at strain ε and temperature T, $E_0(T)$ the small strain modulus at temperature T and ε_y the yield strain holds to a good approximation for both PMMA and PS. The strain involved in the DMTA tests is ~10^{-2} and therefore the storage modulus from the DMTA tests gives a reliable value for E_0.

The stress–strain data gathered over four decades of strain rate indicated that the total strain in the sample rather than the elastic stored energy is the factor which controls compressive failure in PMMA and PS.

In the Ree–Eyring method, adopted by some authors [15, 17] to explain the behaviour of PMMA it is assumed that two rate processes occurred with α dominant at lower rates and β at higher rates. In that formulation only two activation energies are calculated which are the α activation energy ΔG_α and the

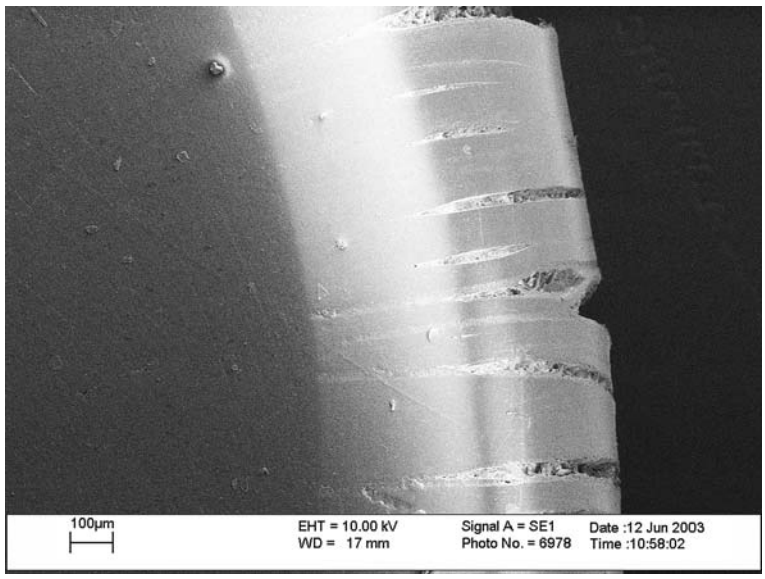

Fig. 11 Electron microscope image of the surface of PMMA compressed to a strain of 0.8. The central band shows a section of the cracked/crazed ring formed around the sample, the region to the left is deformed but uncrazed polymer

β activation energy ΔG_β. Bauwens-Crowet [17] found that ΔG_α and ΔG_β to be 412 and 107 kJ mol^{-1} respectively; Roetling [15] 339 and 100 kJ mol^{-1} respectively. Deutsch et al. [22] from tensile modulus measurements obtained a value of 334 kJ mol^{-1} for ΔG_α. From dielectric measurements, De Brouchere et al. [23] reported the values of ΔG_α and ΔG_β to be near 419 kJ mol^{-1} and about 84–96 kJ mol^{-1} respectively. From the calculations in this study, ΔG_y is found in the range 82–126 kJ mol^{-1}, $\Delta G_{20\%}$ 81–161 kJ mol^{-1} and $\Delta G_{30\%}$ 81–119 kJ mol^{-1} for the range of ln($\dot{\varepsilon}$) from −5.5 to 0.3 (strain rate: 0.004–1.3 s^{-1}). These values are of similar magnitudes to those obtained by previous workers for ΔG_β using alternative analysis techniques. In the analysis used here the values obtained for υ_a show a continuous change with strain and temperature. The increase in activation volume with increasing strain may perhaps be interpreted as an increase in the distance between equilibrium positions for polymer chain conformation with increasing strain.

For PS the DMTA data showed that, as expected, the α relaxation temperature (T_g) increased with rate showing a rate sensitivity of ~7° per decade. The β relaxation however had a much greater sensitivity (~35° per decade) and increased with strain rate merging into the α relaxation at strain rates >1 s^{-1}.

References

1. Crawshaw J, Sferrazza M, Donald AM (2001) Plast Rubber Compos 30(2):68
2. Arakawa K, Takahashi K (1997) Int J Fract 86(4):289
3. Ward IM (1971) J Mater Sci 6:1397
4. Bauwens JC (1970) J Polym Sci, Part A-2 8:893
5. Bowden PB, Jukes JA (1973) J Mater Sci 7:52
6. Hall IH (1968) J Appl Polym Sci 12:739
7. Fleck NA, Stronge WJ, Liu JH (1990) Proc Roy Soc Lond A429:459–479
8. Lerch V, Gary G, Herve P (2003) J Phys IV 110:159
9. Walley SM, Field JE, Pope PH, Safford NA (1989) Phil Trans Roy Soc Lond 328A:1
10. Swallowe GM, Fernandez JO (2000) J Phys IV France 10:311
11. Illers KH (1961) Z Elecktrochem 65:679
12. Illers KH, Jenckel E (1959) J Polym Sci 41:528
13. Halsey G, White HJ Jr, Eyring H (1945) Textile Res J 15:295
14. Ree T, Eyring H (1958) In: Eirich FR (ed) Rheology, vol II, Chapter III. Academic Press, New York
15. Roetling JA (1965) Polymer 6:311
16. Bauwens-Crowet C, Bauwens JC, Homes G (1969) J Polym Sci A-2 7:735
17. Bauwens-Crowet C (1973) J Mater Sci 8:968
18. Zhu XX, Zhu GR (1992) Polymer 33:4968
19. Nanzai Y (1990) Polym Eng Sci 30:96
20. Bauwens-Crowet C, Ots J-M, Bauwens J-C (1974) J Mater Sci Lett 9:1197
21. Argon AS (1973) Phil Mag 28:839
22. Deutsch K, Hoff EAW, Reddish W (1954) J Polym Sci 13:565
23. De Brouchere L, Offergeld G (1958) J Polym Sci 30:105